Simulation of capillary flow with a dynamic contact angle

van Mourik, S; Veldman, AEP; Dreyer, ME

Published in:
Microgravity science and technology

Publication date:
2005

S. van Mourik[1,2], A.E.P. Veldman[2] and M.E. Dreyer[3]

Simulation of Capillary Flow with a Dynamic Contact Angle

A number of theoretical and empirical dynamic contact angle (DCA) models have been tested in a numerical simulation of liquid reorientation in microgravity for which experimental validation data are available. It is observed that the DCA can have a large influence on liquid dynamics in microgravity. Correct modelling of the DCA is found to be essential for realistic numerical simulation, and hysteresis effects cannot be ignored.

1 Introduction

Sloshing of liquid onboard spacecraft, e.g. fuel or cargo, can produce unwanted disturbances of the spacecraft motion. These can jeopardize the success of manoeuvres such as docking, which require millimeter precision. A recent example of a mission that was seriously influenced by 'overenthousiastic' liquid behaviour was NEAR (Near Earth Asteroid Rendezvous). During a course correction the NEAR spacecraft shut itself down, and it was difficult to regain control. Reconstruction of the incident learned that during the orbital manouevre the propellant liquid reacted more dynamic than anticipated: it came outside the foreseen operational envelope and the spacecraft went into a safety mode. The NEAR mission suffered a 13 month delay due to this incident [1, 2].

To control spacecraft dynamics, insight is required in the behaviour of liquid under conditions where capillary forces dominate over gravity, as in microgravity. A 'classical' treatise on sloshing in spacecraft has been prepared by Abramson [3] (in particular, see Chapter 11). As just indicated, a major physical ingredient of liquid motion onboard satellites are the capillary forces. These include surface tension effects along the liquid surface, as well as wetting properties and the associated contact line dynamics. Here, the contact angle (i.e. the angle between the free liquid surface and the confining wall) plays an important role. It determines the motion of the contact line, and herewith the global liquid dynamics. In gravity, the influence of the contact angle is often negligible and therefore it does not have to be modelled accurately for reliable predictions of liquid motion. However, in microgravity this is not the case, and a detailed study of the contact angle and the related contact line motion is required.

When a liquid is brought into contact with a solid surface, adhesion of the liquid with the solid and with the ambient air, and cohesion of the liquid become interacting forces; the contact angle is a result of the three-phase balance of these forces. When the force balance is in equilibrium, the contact line does not move; the matching contact angle is then called static. If the force balance is out of equilibrium, the contact line will move towards its equilibrium position. Contact line motion has long been badly understood, because on a continuum scale a viscous liquid cannot move along a solid surface (the no-slip condition), see e.g. the review article by Dussan V. [4]. Experimental observations reveal that the contact line motion takes place on a microscopic molecular scale, where the liquid is rolling along the solid surface. These observations have recently been given a theoretical explanation [5]. On a global hydrodynamic scale, the contact line motion induces an apparent or macroscopic (dynamic) contact angle (DCA). When the liquid comes to rest the macroscopic contact angle equals the static contact angle (SCA).

Authors:
[1] Present address: Department of Applied Mathematics
University of Twente, Enschede.

[2] Institute of Mathematics and Computing Science
University of Groningen, P.O. Box 800, NL-9700 AV Groningen
The Netherlands

[3] Center of Applied Space Technology and Microgravity
University of Bremen,
Am Fallturm, D-28359 Bremen, Germany

Paper submitted. 16.12.05
Submission of Final Revised Version: 21.05.05
Paper finally accepted: 23.05.05

The velocity with which the contact line moves is called the contact line velocity (V_{CL}); it often can be modelled as a function of the DCA; e.g. [4] or [6]. Several investigations have been made to relate the V_{CL}, represented by the capillary number, to the discrepancy between DCA and SCA. Many of these investigations are empirically based, and cover only small capillary numbers. Three of these empirical models will be inspected more closely, namely those of Jiang et al. [7], Bracke et al. [8] and Seeberg et al. [9]. The experimental data these models are based on show a large scattering. This is of course partly due to error in measurement and/or experiment, but theoretical work suggests that more parameters play an explicit role in the kinetics of the DCA, for example the surface structure of the solid and the type of liquid [6].

Attempts have been made from various scientific perspectives to obtain theoretical understanding of the DCA. E.g. research based on molecular kinetics has been carried out by Blake since the mid 1970s, see e.g. [6]. A new theory, derived from first principles, that relates the microdynamic physics close to the contact line to the macrodynamic hydrodynamics has been presented by Shikhmurzaev [5]. In particular, his theory predicts the rolling contact line motion that was found experimentally. As examples of other approaches, Fan et al. [10] discuss a thermodynamic point of view, whereas Zhang and Kwok [11] discuss a Lattice-Boltzmann model.

In the present paper, the consequences of Blake's theoretical model, and the empirical models of Jiang, Bracke, and Seeberg for computational fluid dynamic simulations in microgravity are investigated. Especially, we are interested in the dependence of the liquid dynamics on the modelling of the DCA. In concreto, the flow in a partially liquid-filled axisymmetric tube is considered after a step reduction of gravity (Fig. 1). Experimental validation data are available for two different liquids: one with a large and one with a small SCA. The experimental results have been obtained in the ZARM drop tower of the University of Bremen [12, 13].

2 Mathematical model

2.1 Equations of motion

The above-mentioned contact line models will be compared in a computational study of liquid reorientation in microgravity. The flow model is based on the incompressible Navier-Stokes equations, consisting of conservation of mass

$$\nabla \cdot \mathbf{u} = 0, \tag{1}$$

and conservation of momentum

$$\frac{\partial \mathbf{u}}{\partial t} + \nabla \cdot \left(\mathbf{u}\mathbf{u}^{\mathrm{T}}\right) = -\frac{1}{\rho}\nabla \mathbf{p} + \frac{\mu}{\rho}\nabla^2 \mathbf{u} + \mathbf{F}. \tag{2}$$

Here, $\mathbf{u}$ denotes velocity, ρ density, p pressure and μ molecular viscosity; $\mathbf{F}$ represents an external force (e.g. gravity).
Equations (1) and (2) have to be supplied with boundary conditions. At a solid wall a no-slip condition $\mathbf{u} = \mathbf{0}$ is prescribed, however the contact line is allowed to move, as will be discussed below. At the free liquid surface continuity of normal and tangential stress is imposed:

$$-p + 2\mu \frac{\partial u_n}{\partial n} = -p_0 + 2\gamma H, \tag{3}$$

$$\mu\left(\frac{\partial u_n}{\partial t} + \frac{\partial u_t}{\partial n}\right) = 0. \int \tag{4}$$

Here, u_n and u_t are the velocity components normal and tangential to the free surface, with n and t the corresponding directions. Further, p_0 denotes the atmospheric pressure, γ surface tension and $2H$ the total curvature of the free surface. Also, a kinematic condition describing the evolution of the free surface is present,

$$\frac{DG}{Dt} \equiv \frac{\partial G}{\partial t} + \mathbf{u} \cdot \nabla G = 0. \tag{5}$$

stating that liquid only moves through advection. $G(x, t)$ is an indicator function with $G(x, t) = 1$ when liquid is present at position x and time t, otherwise $G(x, t) = 0$. Finally, to complete the system of hydrodynamic equations, the macroscopic contact angle has to be prescribed; this will be discussed below.

2.2 Contact angle models

Dynamic contact angle: The theoretical studies on wetting carried out in the last decades (Shikhmurzaev [14] gives a comprehensive discussion) have led to a number of theoretical dynamic contact angle models. In all of these models the contact line is allowed to move along the solid surface. For the contact line velocity various proposals have been made. To 'circumvent' the no-slip condition of the flow on a macro scale, it is generally assumed that the liquid near the contact line is rolling over the solid surface [5].

In our numerical simulations we have applied the model of Blake [6], which is based on molecular kinetics. This model has also been investigated elsewhere, e.g. in an experimental study by Hamraoui et al. [15]. To describe this model, first let $\theta(t)$ denote the dynamic contact angle, and θ_0 its (static) equilibrium

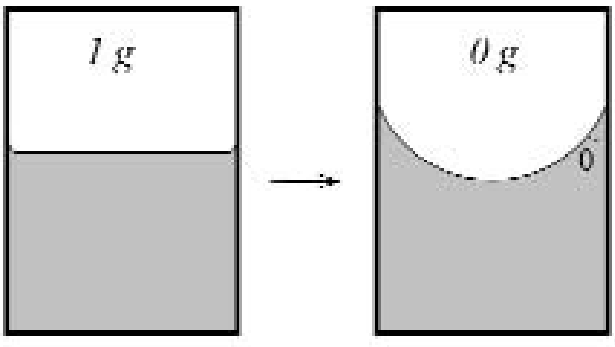

Figure 1: Liquid reorientation after a step reduction of gravity.

value. Then Blake's model [6] is formulated as

$$V_{CL} = A \sinh B(\cos\theta_0 - \cos\theta(t)), \tag{6}$$

where $A = 2\kappa_s^0 \lambda\hbar/(\mu v)$ and $B = \gamma/(2nkT)$, with κ_s^0 the frequency of molecular displacements at equilibrium, λ the average length of an individual molecular displacement in the three-phase zone, $\hbar$ Planck's constant, v the molecular flow volume, n the number of adsorption sites per unit area, κ Boltzmann's constant and T the temperature. For many liquids the values of these parameters are known.

In contrast with the theoretical studies, also dynamic contact angle models have been proposed that are based on experimental measurements. These models are formulated in terms of the capillary number

$$\mathrm{Ca} \equiv \frac{\mu V_{CL}}{\gamma}, \quad \text{i.e.} \quad \frac{\text{viscous forces}}{\text{capillary forces}}. \tag{7}$$

We will consider three of these empirical models, in chronological order given by

- Jiang et al. [7]

$$\tanh\left(4.69\,\mathrm{Ca}^{0.702}\right) = \frac{\cos\theta_0 - \cos\theta(t)}{\cos\theta_0 + 1}; \tag{8}$$

- Bracke et al. [8]

$$2\mathrm{Ca}^{0.5} = \frac{\cos\theta_0 - \cos\theta(t)}{\cos\theta_0 + 1}; \tag{9}$$

- Seeberg et al. [9]

$$2.24\mathrm{Ca}^{0.54} = \frac{\cos\theta_0 - \cos\theta(t)}{\cos\theta_0 + 1}. \tag{10}$$

Recently, Billingham [16] proposed a similar relation where the contact line velocity is considered a linear function of the contact angle (for a static angle of 90°). He found that the influence of the proportionality constant is quite substantial. Wölk et al. [17] followed a different approach, where the contact angle is proposed a function of the deviation from the equilibrium height. Again another approach to simulate the contact line dynamics is through Lattice Boltzmann modelling [11]. It is interesting to note that this microscale approach is able to very accurately predict Blake's macroscale model (6). It should be stressed that the empirical models (8)–(10) are only valid for positive contact line velocity, i.e. for an advancing contact line, whereas Blake's model (6) is generally applicable, for advancing as well as for receding contact lines.

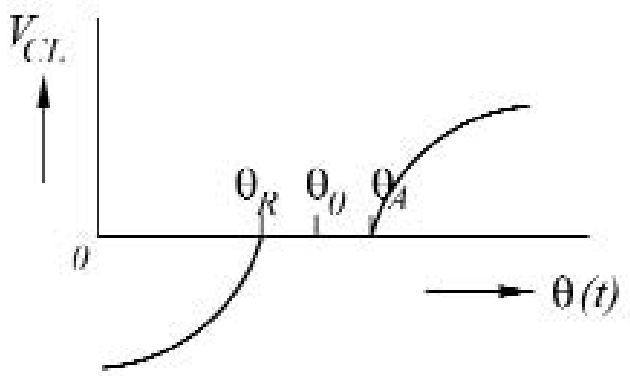

Figure 2: Schematic contact line velocity with hysteresis.

Hysteresis: In theory, the contact line velocity V_{CL} is equal to zero if and only if $\theta(t) = \theta_0$, which is in practice often not the case. This phenomenon is called contact angle hysteresis, and is generally attributed to surface roughness of the solid (see [4], [6] and references therein). The result is that the contact line stops moving already when it is close to its equilibrium position (Fig. 2). The V_{CL} is then equal to zero in an interval $[\theta_R, \theta_A]$ which is called the hysteresis domain. The angles θ_R and θ_A are called the receding and advancing contact angle, respectively. A theoretical manner to model the hysteresis domain is not known to the authors, but for some liquids experimental data are available [12, 13].

3. Numerical method

The equations of motion as given in Section 2, written in an axisymmetric formulation, have been solved with a finite-volume method on a Cartesian staggered grid. If required, nonuniform grids have been employed; to evaluate the numerical discretization error grid refinement studies have been carried out. The position of the free liquid surface has been described with a VOF[18]-based method. Its evolution is governed in principle by Eq. (5). The numerical evolution follows a mass-conservative displacement algorithm. Adaptions to the evolution described in [18] have been made to prevent the 'flotsam' and 'jetsam' from which the original VOF formulation suffers. An essential ingredient is the use of a local height function to describe the free surface position. Details of the numerical method can be found in [19]–[23].

4. Experiment

To validate the dynamic contact angle models, two experiments carried out in the 145 *m* high drop tower of the ZARM institute in Bremen have been simulated [12, 13]. The experiments involve a (partially) liquid-filled axisymmetric cylindrical tube that is released from the tower, after which it experiences a period of 4.74 seconds of free fall. The liquid velocities, e.g. the contact line velocity V_{CL}, are kept relatively low by means of a small tube radius, resulting in a low capillary number $\mathrm{Ca} \equiv \mu V_{CL}/\gamma$, implying that viscous forces are relatively unimportant in comparison with capillary forces (see Eq. (7)). The values for the Ohnesorge number $\mathrm{Oh} \equiv (\upsilon^2\rho/\gamma R)^{1/2}$, lying well below 10^{-2} (see Table 1), also indicate only a minor role of the viscosity. Under terrestrial gravity, the Bond numbers $\mathrm{Bo} \equiv \rho g R^2/\gamma$ for the

	M3	detra
radius of test tube (m)	$1.0\ 10^{-2}$	$1.5\ 10^{-2}$
viscosity μ/ρ (m^2/s)	$2.91\ 10^{-6}$	$2.51\ 10^{-6}$
surface tension γ/ρ ($m^3/s2$)	$2.06\ 10^{-5}$	$2.97\ 10^{-5}$
static contact angle θ_0 (deg)	53.6°	5.5°
Bond number (earth)	47.6	74.3
Ohnesorge number	$6.41\ 10^{-3}$	$3.77\ 10^{-3}$

Table 1: Some experiment parameters and corresponding dimensionless numbers.

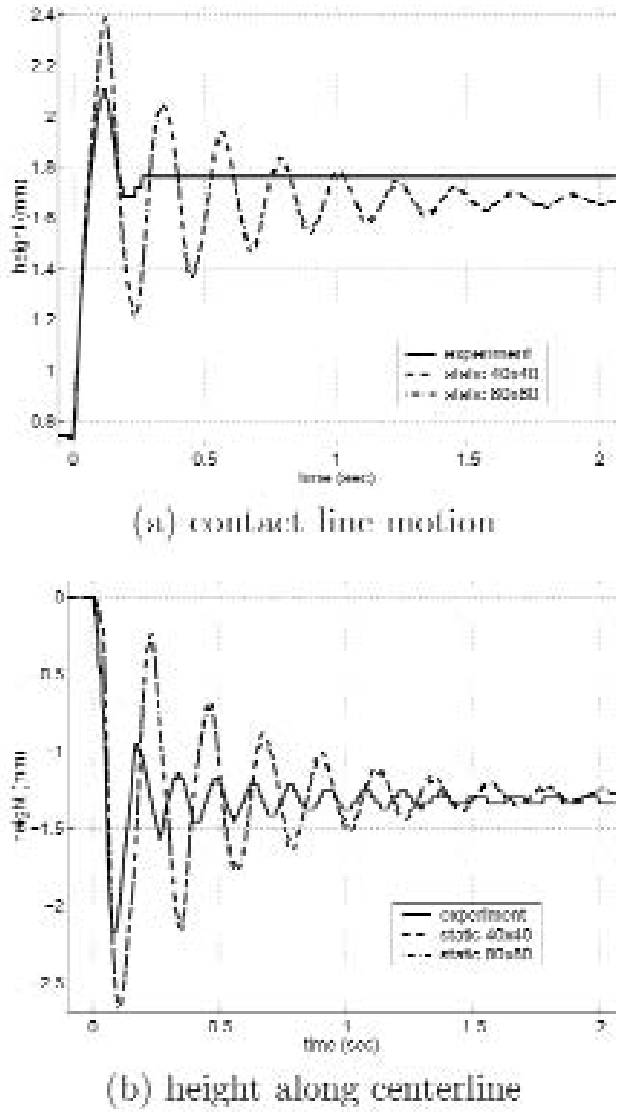

Figure 3: Free surface motion with a static contact angle vs. experiment: a) contact line motion, b) height along centerline.

experiments range from 47 to 74. This number indicates the relative influence of gravity over capillary effects.

The response of the contact line and of the liquid height at the centerline of the tube is monitored during the experiment. Initially, under gravity the liquid surface is (almost) flat; then, during the free fall, the liquid surface turns into a spherical shape specified by the static contact angle. The experiments involve two types of liquid: one liquid (M3) with a large SCA, and one liquid (detra) with a small SCA. Table 1 gives some relevant physical data [12, 13].

5. Results

In this section the results of the numerical simulations will be reported and compared with the experimental results. The alternatives from Section 2.2 for modelling the contact angle have been investigated: the static contact angle $\theta = \theta_0$, Blake's theoretical model (6), and the three empirical models (8)–(10). Each of these models has a local character and can be implemented in quite general conditions, e.g. irrespective of wall geometry. Also the effect of wall roughness leading to hysteresis is studied. The comparison with experiment is made in terms of the position of the contact line along the side wall of the tube as a function of time, and the height of the free surface along the centerline. (Note that the initial centerline position is used as the reference position $h = 0$.)

5.1 Large static contact angle

To begin with, we report on the experiments with Baysilone M3, a silicon oil manufactured by Bayer AG. In this experiment, the cylinder wall was covered with a thin sheet of FC- 732 to produce contact angles away from zero degrees: experimentally the contact angle was determined at 53.6° ± 1.6°. The physical parameters pertinent to Blake's model can be found in [6]; however, these were determined for a different solid wall material. In all simulations, first the equilibrium position under gravity was calculated. From that initial condition, gravity was instantaneously removed, mimicing the free fall in the drop tower.

Static contact angle: In the first simulation a static contact angle is used. In this model, the contact line is moved such that at all times $\theta = \theta_0$. This is a simple model, which conceptually differs from the dynamic contact angle models discussed in Section 2.2. Comparison with experiment in Fig. 3a shows that the contact line starts moving too violent, and furthermore it keeps moving for too long. Also, consistently, along the centerline the liquid keeps oscillating much too long (Fig. 3b). The simulations have been carried out for two different computational grids, 40×40 and 80 × 80, revealing that the numerical discretisation error is quite modest. Clearly, a static contact angle does not fit the flow dynamics.

Blake's model: Next Blake's model (6) has been implemented,

at first without hysteresis. For a silicon oil moving along a glass surface, Blake [6] gives physical values for the parameters that appear in his model: $k_s^0 = 1.7\ 10^{11}\ s^{-1}$, $\lambda = 0.8\ 10^{-9}$ m/s, $\nu = \lambda^3$, $n = 1.6\ 10^{18}\ m^{-2}$ and we assume that $T = 293°$ K.

These values lead to $A = 1.4\ 10^{-1}$m/s and $B = 1.3$. The results are shown in Fig. 4. The maximum wall height is very nicely predicted now, but the liquid still keeps on moving for too long (Fig. 4a), although it damps more than with the static model. On the other hand, the motion along the centerline seems to damp out too much (Fig. 4b). Again, this difference cannot be blamed to numerical discretization errors: the 40 × 40 and 80 × 80 computational grids produce almost indistinguishable results. The experiment gives the impression that the contact line gets stuck. Thus it was decided to add hysteresis to the model. Michaelis and Dreyer [13] have actually measured the receding and advancing contact angle. For M3 they found $\theta_R = 46.7° \pm 2.1°$, $\theta_0 = 53.6° \pm 1.6°$ and $\theta_R = 56.4° \pm 1.0°$.

The dashed curve in Fig. 5 shows that the contact line motion is now predicted much closer to the experiment. Further, the height along the centerline is oscillating much longer than without hysteresis (compare the dashed curve in Fig. 5b with Fig. 4b); this behaviour is compatible with the experimental observations. A similar oscillating behaviour of the centerline height in the presence of a stuck contact line has been observed in [13].

The solution turns out somewhat sensitive to the chosen hysteresis domain. It allows, within the experimental uncertainty range, to choose the contact angles such that even a better fit with experiment results, both in contactline motion as in the free-surface height along the centerline. This also is shown in Figure 5, where the dash-dotted curve represents the outcome for $\theta_R = 48.5°$, $\theta_0 = 55.0°$ and $\theta_R = 55.4°$.

Empirical models: As the empirical DCA models (8)–(10) are restricted to an advancing contact line, only the first advancing phase of the contact line motion can be simulated. Fig. 6 shows a comparison with Blake's results and with experiment (note that hysteresis does not yet come into play in this initial phase). Blake's theoretical, and generally applicable, model fits the experiments somewhat better than the empirical models (recall the large experimental scattering these models are based on). The behaviour is consistent with the theoretical relation between capillary number and contact angle, as plotted in Fig. 7. When the DCA remains under 65°, which is the case here, the theoretical velocity profiles imply that Blake's model predicts the highest initial contact line velocity, followed by Jiang, Seeberg and Bracke, respectively. This ordering is also found in the computational results in Fig. 6.

5.2 Small static contact angle

The second liquid that has been used for experiment has a very small SCA (5.5°). This means that in order to reach equilibrium position, the contact line has to rise considerably from its equilibrium height in gravity, in contrast with the M3 experiment. Another difference with M3 is that the small SCA brings along a numerical difficulty: when the liquid is at rest, with or without gravity, the liquid surface near the wall is highly curved. This causes a significant error in the discretisation of the contact angle when the uniform M3 grid is used. However, this error is reduced considerably with local grid refinement near the wall. Additionally, a numerical correction has been applied which transforms the analytical contact angle at the wall to an average contact angle over the grid cell adjacent to the wall. It has been verified that with these adjustments, in absence of gravity (which is the most critical situation) the discrete equilibrium height matches its analytical value. For details we refer to [20]. Two different grids of 40 × 60 and 80 × 120 cells show that also for this test case the numerical discretisation error is quite modest (Figs. 8 and 10). Further, no hysteresis is modelled in this test case, because the contact line keeps advancing throughout the experiment.

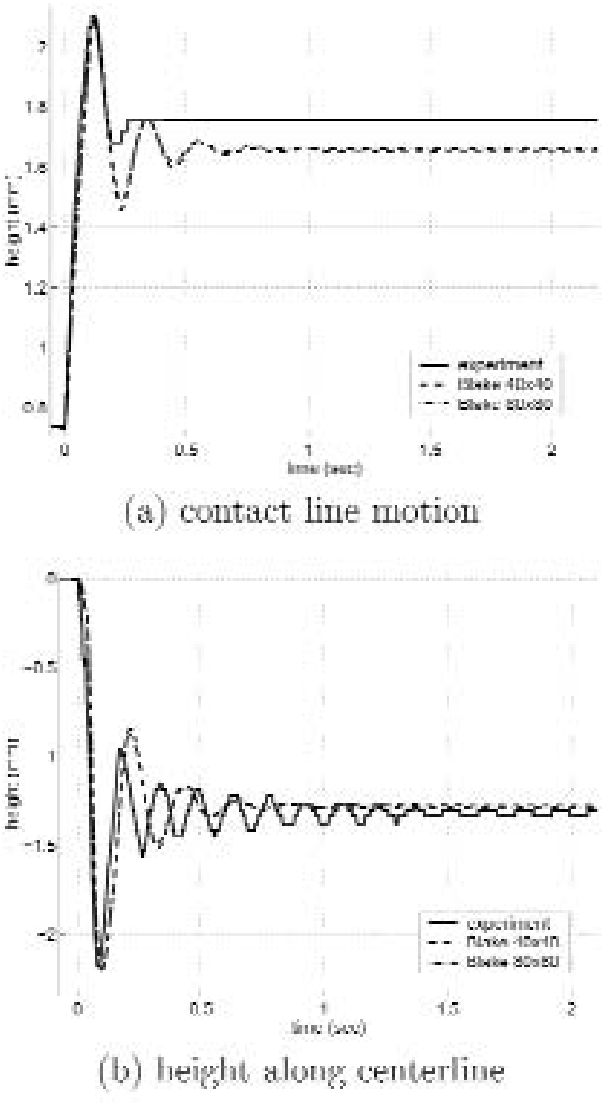

Figure 4: (a) Contact line motion and (b) height along centerline for M3 with Blake´s Model vs. experiment.

Static model: The reorientation results for the static contact angle model are shown in Fig. 8. As in the previous test case, in the early reorientation phase the computed V_{CL} is much too high compared to experiment.

Blake's model: Detra is a mixture of five volumes 1234-tetrahydronaphtalene and eight volumes decahydronaphtalene [12]. The values for λ and κ_ω^0 in coefficient A in (6) could not be found by the authors. It is instructive to see what happens if, for example, these unknown values are chosen to have the same values as for M3; this leads to $A = 1.6\ 10^{-1}$ m/s and $B = 2.1$. Figure 9 shows that the initial contact line velocity is much too high, unlike the M3 situation, which stresses the importance of a correct parameter choice. Subsequently, the coefficient A has been adjusted to fit the experimental results; this yielded $A = 4.3\ 10^{-2}$ m/s. Figure 10 shows that now Blake's model is much better.

Comparison with the other models: Figure 11 gives the results of the empirical models, compared to Blake's model. Because no negative contact line velocities occur, the three empirical models are applicable throughout (in contrast with the situation with a large contact angle in the previous section). Right after $t = 0$, the empirical models give rise to a very high contact line velocity, and after that the contact line almost stops moving. None of them resembles experiment very well. This is in contrast with the contact line from Blake's theoretical model, which follows the experimental contact line much better. The computational results in Fig. 11 match the theoretical velocity profiles in Fig. 12. For the large contact angles that appear in the initial reorientation phase, Blake predicts a much smaller velocity than

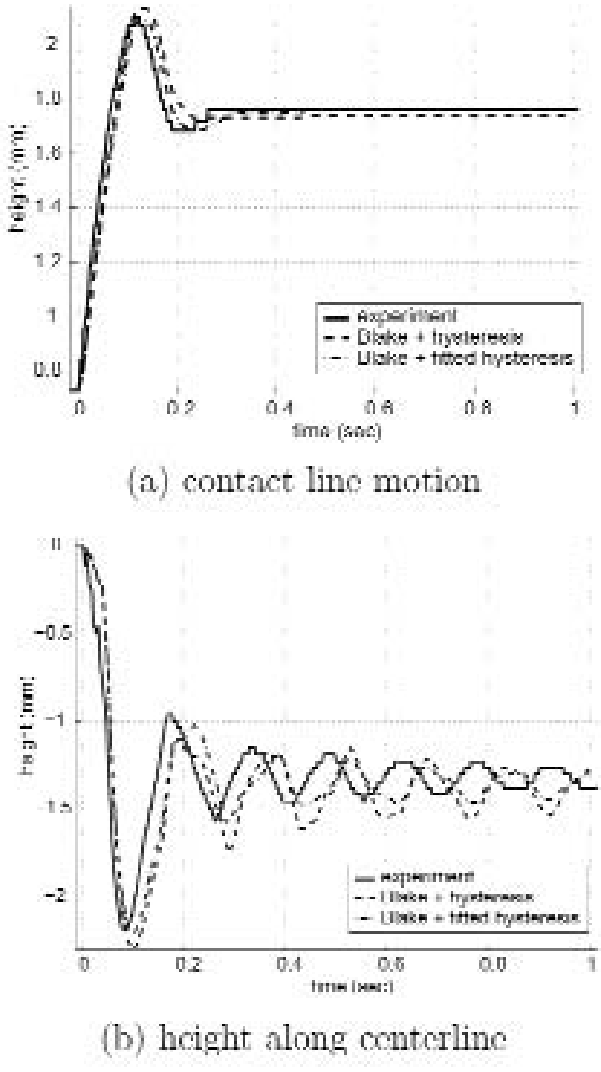

Figure 5: Hysteresis added to Blake's model: (a) contact line motion and (b) height along centerline. The hysteresis domain has been chosen according to the measurements in [13]; the fitted values are chosen within the experimental uncertainty range.

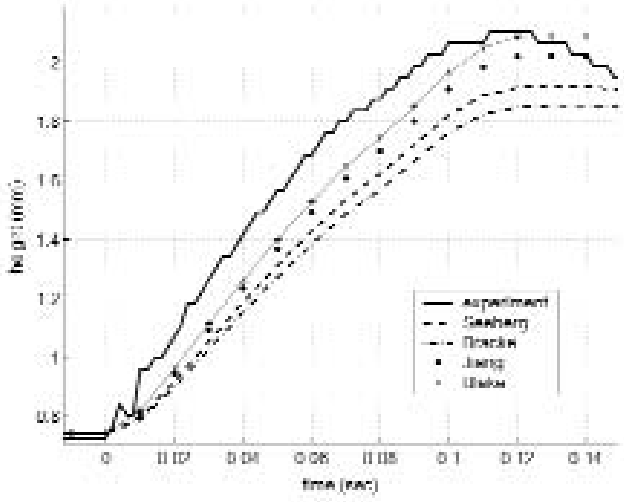

Figure 6: Validation of contact line motion for M3: Blake's theoretical model compared with three empirical models.

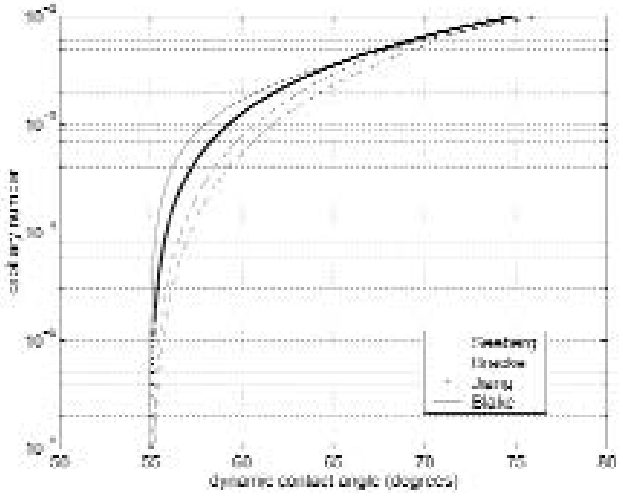

Figure 7: Theoretical velocity profiles (for M3) corresponding with the various contact line models.

the other models. Figure 12 also shows that within the empirical models Jiang's model predicts the highest V_{CL}, followed by Seeberg and Bracke, respectively, which again is consistent with the computational results in Fig. 11.

6. Discussion

Various, generally implementable, dynamic contact angle models have been tested by means of numerically simulating a number of experiments, in which the reorientation of two liquids, each with different contact angle properties, has been monitored after a step reduction of gravity. It has been shown that the modelling of the DCA can have a large influence on the simulation of liquid dynamics in capillary-dominated situations, such as microgravity.

A first conclusion is that a static contact angle model produces highly inaccurate results. In particular, the liquid reacts too violently and keeps oscillating too long.

Secondly, the use of a dynamic contact angle leads to more realistic results. The theoretical model of Blake [6] works quite well, both for a large and a small contact angle, although in the latter case some of the involved physical parameters were not available and have been chosen to fit the experiment. The oscillating test case with a large contact angle does require the addition of hysteresis. Doing so, with experimentally obtained hysteresis angles, the flow dynamics are accurately captured. We stress that the simulation of the latter flow case only makes use of known physical parameters - no numerical tuning is applied. Thirdly, the investigated empirical models, which are only

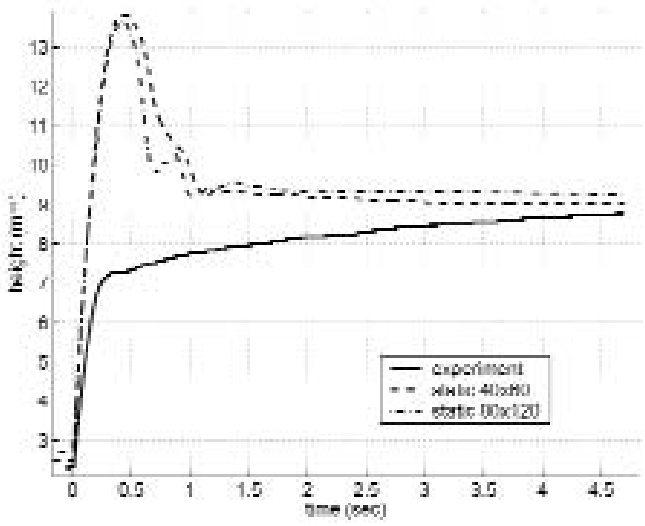

Figure 8: Contact line motion for detra with a static contact angle.

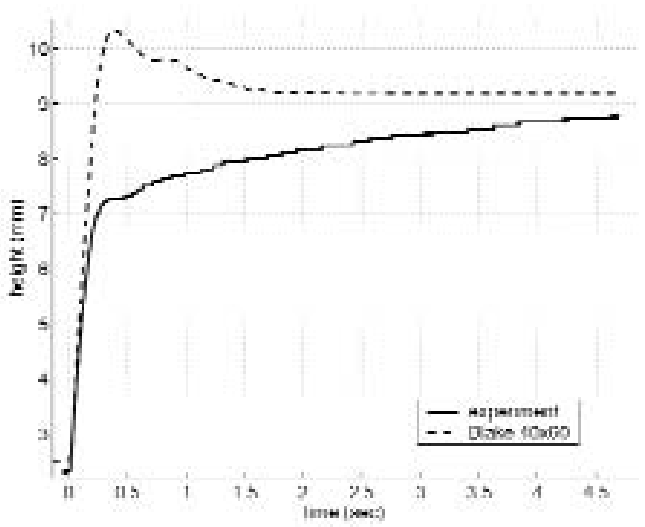

Figure 9: Contact line motion for detra: Blake's model with the coefficient A at its M3 value.

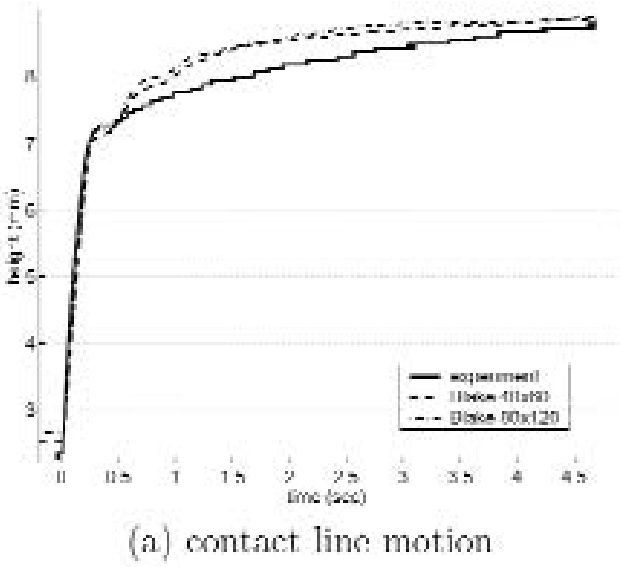

Figure 10: (a) Contact line motion and (b) centerline height for detra: Blake's model with the adjusted coefficient A.

applicable during advancing contact line motion, are less accurate than Blake's model. These models are based on quite scattered experimental data, in contrast with Blake's theoretical basis. The differences between the models can be explained in terms of the relation between contact angle and capillary number. Overall, using Blake's theoretical dynamic contact angle model with a corresponding hysteresis domain, it has been possible to reproduce the experimentally observed contact line behaviour. Thus, it seems promising to further investigate theoretical contact line models (including hysteresis), and to implement them in numerical simulation methods.

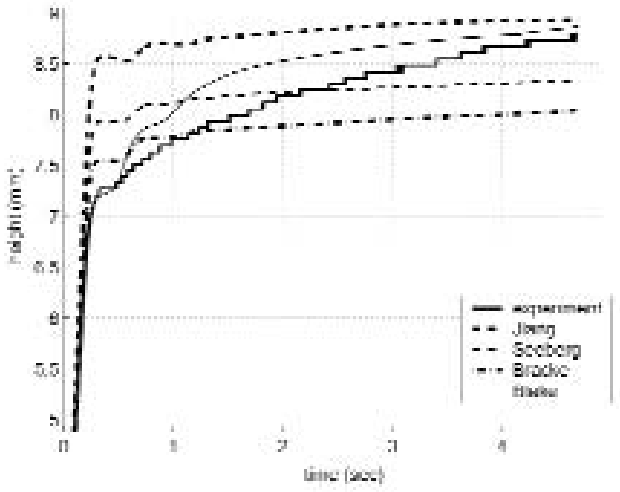

Figure 11: Validation of contact line motion for detra: Blake's theoretical model compared with three empirical models.

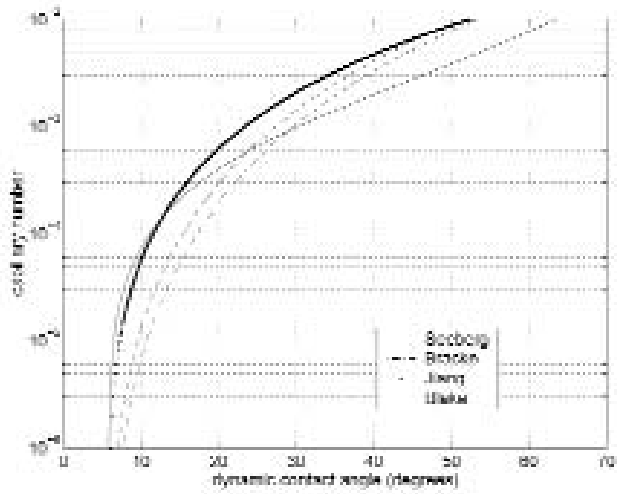

Figure 12: Theoretical velocity profiles (for detra) corresponding with the various contact line models.

References

[1] *H. Worth*: NEAR team recovers mission after faulty engine burn. Available at http://near.jhuapl.edu/news/articles/99jan29 1 (1999).

[2] *NEAR Anomaly Review Board:* The NEAR Rendezvous burn anomaly of December 1998. Johns Hopkins University, Applied Physics Laboratory (November 1999).

[3] *Abramson, H.N. (Ed.):* The dynamic behaviour of liquids in moving containers. NASA SP-106, Washington DC (1966).

[4] *Dussan V., E.B.:* On the spreading of liquids on solid surfaces: static and dynamic contact lines. Ann. Rev. Fluid Mech., vol. 11, p 371–400 (1979).

[5] *Shikhmurzaev, Y.D.:* The moving contact line on a smooth solid surface. Int. J. Multiphase Flow, vol. 19, p. 589–610 (1993).

[6] *Blake, T.D.:* Dynamic contact angles and wetting kinetics. In: Wettability, Berg, J.C. (Ed.), Marcel Dekker, New York, p. 251–309 (1993)

[7] *Jiang, T.S., Oh, S.G., Slattery, J.C.:* Correlation for dynamic contact angle. J. Colloid Interface Sc., vol. 69, p. 74–77 (1979).

[8] *Bracke, M., De Voeght, F., Joos, P.:* The kinetics of wetting: the dynamic contact angle. Progr. Colloid Pol. Sc., vol. 79, p. 142–149 (1989).

[9] *Seeberg, J.E., Berg, J.C.:* Dynamic wetting in the flow of capillary number regime. Chem. Eng. Sc., vol. 47, p. 4455–4464 (1992).

[10] *Fan, H., Gao, Y.X., Huang, X.Y.:* Thermodynamics modelling for moving contact line in gas/liquid/solid system: capillary rise problem revisited. Phys. Fluids, vol. 13, p. 1615–1623 (2001).

[11] *Zhang, J., Kwok, D.Y.:* Lattice-Boltzmann study on the contact angle and contact line dynamics of liquid-vapour interfaces. Langmuir, vol. 20, p. 8137–8141 (2004).

[12] *Michaelis, M.:* Kapillarinduzierte Schwingungen freier Flüssigkeitsoberflächen. Fortschritt- Bericht VDI 454, VDI Verlag, Düsseldorf (2003).

[13] *Michaelis, M., Dreyer, M.E.:* Test-case number 31: reorientation of a free liquid interface in a partly filled right circular cylinder upon gravity step reduction. Multiphase Science and Technology vol.,6p.219-238 (2004).

[14] *Shikhmurzaev, Y.D.:* Moving contact lines in liquid/liquid/solid systems. J. Fluid Mech., vol. 334, p. 211–249 (1997).

[15] *Hamraoui, A., Thuresson, K., Nylander, T., Yaminsky, V.:* Can a dynamic contact angle be understood in terms of a friction coefficient? J. Colloid Interface Sc., vol. 226, p. 199–204 (2000).

[16] *Billingham, J.:* Nonlinear sloshing in zero gravity. J. Fluid Mech, vol. 464, p. 365–391 (2002).

[17] *Wölk, G., Dreyer, M., Rath, H.J., Weislogel, M.M.:* Damped oscillations of a liquid/ gas surface upon step reduction in gravity. J. Spacecraft Rockets, vol. 34, p. 110–117 (1997).

[18] *Hirt, C.W., Nichols, B.D.:* Volume of Fluid (VOF) method for the dynamics of free boundaries. J. Comput. Phys., vol. 39, p. 201–225 (1981).

[19] *Gerrits, J.:* Dynamics of liquid-filled spacecraft. PhD thesis, University of Groningen (2001). Available at www.ub.rug.nl/ eldoc/dis/science/j.gerrits

[20] *Van Mourik, S.:* Numerical modelling of the dynamic contact angle. Master's thesis, University of Groningen (2002).

[21] *Gerrits, J., Veldman, A.E.P.:* Dynamics of liquid-filled spacecraft. J. Eng. Math., vol. 45, p. 21–38 (2003).

[22] *Verstappen, R.W.C.P., Veldman, A.E.P.:* Symmetry-preserving discretisation of turbulent flow. J. Comput. Physics, vol. 187, p. 343–368 (2003).

[23] *Kleefsman, K.M.T., Fekken, G., Veldman, A.E.P., Iwanowski, B., Buchner, B.:* A Volumeof- Fluid based simulation method for wave impact problems. J. Comput. Physics, vol. 206, p. 363–393 (2005).